immunostained as described. Quantification was achieved by using Image-1 software (Universal Imaging). Positive controls included sections of adrenal medulla, thyroid, pancreas, intestine, ganglia and nerves.

Antisense studies. 100 nM phosphorothioate oligodeoxynucleotides with C-5 propyne modifications at dC and dU (Midland) were reconstituted with 2.5 μg ml^{-1} GS2888 cytofectin[30] (Gilead Sciences) in OptiMEM (Gibco), then incubated with 5×10^5 NCI-H209 or DMS53 cells in 6-well plates for 48 h in growth media. 5×10^4 cells were cytospun per slide. Immunostaining, quantified using MetaMorph software (Universal Imaging), included at least ten cell clusters (over 200 cells) for each marker and oligonucleotide. Experiments were done in triplicate for both cell lines and evaluated in a blind fashion. Oligonucleotides c5p1476 (5′-GGAGCCCACUGCUUU-3′), c5p1232 (5′-UCCCAACGCCACUGA-3′) and c5p25 (5′-UCCUACUAAGGCUGC-3′) correspond to positions 1,476–1,491 and 1,232–1,247 in the hASH1 3′ UTR and 25–40 in the 5′ UTR, respectively; the c5pMiss1 sequence is 5′-GCUACAUCUGGUCGC-3′; c5pMiss2 5′-CACUGAUGCACCUGU-3′.

Received 9 January; accepted 20 February 1997.

1. Campuzano, S. *et al.* Molecular genetics of the achaete-scute gene complex of *D. melanogaster*. *Cell* **40,** 327–338 (1985).
2. Jan, Y. N. & Jan, L. Y. Genetic control of cell fate specification in *Drosophila* peripheral nervous system. *Annu. Rev. Genet.* **28,** 373–393 (1994).
3. Johnson, J. E., Birren, S. J. & Anderson, D. J. Two rat homologues of *Drosophila achaete-scute* specifically expressed in neuronal precursors. *Nature* **346,** 858–861 (1990).
4. Lo, L. C. *et al.* Mammalian *achaete-scute* homolog 1 is transiently expressed by spatially restricted subsets of early neuroepithelial and neural crest cells. *Genes Dev.* **5,** 1524–1537 (1991).
5. Sommer, L. *et al.* The cellular function of MASH1 in autonomic neurogenesis. *Neuron* **15,** 1245–1258 (1995).
6. Guillemot, F. *et al.* Mammalian *achaete-scute* homolog 1 is required for the early development of olfactory and autonomic neurons. *Cell* **75,** 463–476 (1993).
7. Baylin, S. B. & Gazdar, A. F. in *Small Cell Lung Cancer* 123–143 (Grune and Stratton, New York, 1981).
8. Gazdar, A. F. *et al.* Expression of neuroendocrine cell markers L-dopa decarboxylase, chromogranin A, and dense core granules in human tumors of endocrine and nonendocrine origin. *Cancer Res.* **48,** 4078–4082 (1988).
9. Gazdar, A. F. *et al.* in *Small Cell Lung Cancer* 145–177 (Grune and Stratton, New York, 1981).
10. Linnoila, R. I. in *Neuropeptides in Respiratory Medicine* 197–224 (Dekker, New York, 1994).
11. Mabry, M. *et al.* Transitions between lung cancer phenotypes—implications for tumor progression. *Cancer Cells* **3,** 53–58 (1991).
12. Ball, D. W. *et al.* Identification of a human *achaete-scute* homolog highly expressed in neuroendocrine tumors. *Proc. Natl Acad. Sci. USA* **90,** 5648–5652 (1993).
13. Linnoila, R. I. *et al.* Neuroendocrine differentiation in endocrine and nonendocrine lung carcinomas. *Am. J. Clin. Pathol.* **90,** 641–652 (1988).
14. Linnoila, R. I., Piantadosi, S. & Ruckdeschel, J. C. Impact of neuroendocrine differentiation in non-small cell lung cancer. *Chest* **106,** 367S–371S (1994).
15. Linnoila, R. I. & Aisner, S. C. in *Lung Cancer* 73–95 (Wiley-Liss, New York, 1995).
16. Carney, D. N. *et al.* Establishment and identification of small cell lung cancer cell lines having classic and variant features. *Cancer Res.* **45,** 2913–2923 (1985).
17. Pettengill, O. S. *et al.* Isolation and growth characteristics of continuous cell lines from small-cell carcinoma of the lung. *Cancer* **45,** 906–918 (1980).
18. Bergh, J. *et al.* Establishment and characterization of a continuous lung squamous cell carcinoma cell line (U-1752). *Anticancer Res.* **1,** 317–322 (1981).
19. Gazdar, A. F. *et al.* Establishment of continuous, clonable cultures of small-cell carcinoma of lung which have amine precursor uptake and decarboxylation cell properties. *Cancer Res.* **40,** 3502–3507 (1980).
20. Gazdar, A. F. *et al.* Characterization of variant subclasses of cell lines derived from small cell lung cancer having distinctive biochemical, morphological, and growth properties. *Cancer Res.* **45,** 2924–2930 (1985).
21. Brower, M. *et al.* Growth of cell lines and clinical specimens of human non-small cell lung cancer in a serum-free defined medium. *Cancer Res.* **46,** 798–806 (1986).
22. Linnoila, R. I. Spectrum of neuroendocrine differentiation in lung cancer cell lines featured by cytomorphology, markers, and their corresponding tumors. *J. Cell. Biochem.* **24** (suppl.), 92–106 (1996).
23. Falco, J. P. *et al.* v-rasH induces non-small cell phenotype, with associated growth factors and receptors, in a small cell lung cancer cell line. *J. Clin. Invest.* **85,** 1740–1745 (1990).
24. H. C. Chen *et al.* Conservation of the Drosophila lateral inhibition pathway in human lung cancer: a hairy-related protein (HES-1) directly represses achaete-scute homolog-1 expression. *Proc. Natl Acad. Sci. USA* (in the press).
25. Jarriault, S. *et al.* Signalling downstream of activated mammalian notch. *Nature* **377,** 355–358 (1995).
26. Ishibashi, M. *et al.* Targeted disruption of mammalian hairy and enhancer of split homolog-1 (HES-1) leads to up-regulation of neural helix-loop-helix factors, premature neurogenesis, and severe neural tube defects. *Genes Dev.* **9,** 3136–3148 (1995).
27. Gomez-Skarmeta, J. L. *et al.* Araucan and caupolican, two members of the novel iroquois complex, encode homeoproteins that control proneural and vein-forming genes. *Cell* **85,** 95–105 (1996).
28. Nelkin, B. D. *et al.* Transcription factor levels in medullary thyroid carcinoma cells differentiated by Harvey *ras* oncogene: c-jun is increased. *Biochem. Biophys. Res. Commun.* **170,** 140–146 (1990).
29. Broers, J. L. V. *et al.* Expression of c-*myc* in progenitor cells of the bronchopulmonary epithelium and in a large number of non-small cell lung cancers. *Am. J. Resp. Cell Mol. Biol.* **9,** 33–43 (1993).
30. Lewis, J. G. *et al.* A serum-resistant cytofectin for cellular delivery of antisense oligodeoxynucleotides and plasmid DNA. *Proc. Natl Acad. Sci. USA* **93,** 3176–3181 (1996).

Acknowledgements. H.J.K.v.d.V. was a visiting research assistant of the National Fund for Scientific Research, Belgium. We thank F. Guillemot and A. Joyner for the MASH1$^{\Delta}$ mouse strain and for whole mouse embryo sections hybridized with MASH1; R. Wagner for GS2888 cytofectin; A. F. Gazdar for cell lines; E. Gabrielson for a human fetal lung specimen; S. M. Steinberg for statistical consultation; and S. Jensen, T. Bunnag and K. Wieman for technical assistance. Animal care procedures were approved by the Johns Hopkins Animal Care and Use Committee. Supported in part by grants from the NIH, the American Cancer Society and the D. Collen Research Foundation.

Correspondence and requests for materials should be addressed to D.W.B. (e-mail: dball@welchlink.welch.jhu.edu).

Differential activation of transcription factors induced by Ca^{2+} response amplitude and duration

Ricardo E. Dolmetsch*, Richard S. Lewis*†, Christopher C. Goodnow†‡ & James I. Healy†‡

** Department of Molecular and Cellular Physiology and Neurosciences Program, † Program in Immunology, ‡ Department of Microbiology and Immunology and Howard Hughes Medical Institute, Stanford University School of Medicine, Stanford, California 94305, USA*

An increase in the intracellular calcium ion concentration ($[Ca^{2+}]_i$) controls a diverse range of cell functions, including adhesion, motility, gene expression and proliferation[1,2]. Calcium signalling patterns can occur as single transients, repetitive oscillations or sustained plateaux[2,3], but it is not known whether these patterns are responsible for encoding the specificity of cellular responses. We report here that the amplitude and duration of calcium signals in B lymphocytes controls differential activation of the pro-inflammatory transcriptional regulators NF-κB, c-Jun N-terminal kinase (JNK) and NFAT. NF-κB and JNK are selectively activated by a large transient $[Ca^{2+}]_i$ rise, whereas NFAT is activated by a low, sustained Ca^{2+} plateau. Differential activation results from differences in the Ca^{2+} sensitivities and kinetic behaviour of the three pathways. Our results show how downstream effectors can decode information contained in the amplitude and duration of Ca^{2+} signals, revealing a mechanism by which a multifunctional second messenger such as Ca^{2+} can achieve specificity in signalling to the nucleus.

Calcium signalling is important for the growth, death, differentiation and function of immune cells[4–6]. Several Ca^{2+}-sensitive transcriptional regulators, including NF-κB[7,8], JNK[9,10] and NFAT[4,6,11–14], participate in varying combinations to promote the expression of genes that underlie these responses. These genes encode haematopoietic growth factors such as the interleukins IL-2 and IL-4 and GM-CSF, and inflammatory cytokines such as IL-1, IL-6, IL-8 and tumour-necrosis factor (TNF)[4,7,10,14]. We examined the Ca^{2+} sensitivity and response dynamics of the three transcriptional regulators in B lymphocytes from mice expressing an immunoglobulin transgene specific for the hen-egg lysozyme (HEL) antigen[15]. Acute stimulation of B cells with HEL and phorbol ester evoked a biphasic Ca^{2+} response that consisted of an initial rapid rise of $[Ca^{2+}]_i$ from a baseline of 76 ± 3 nM to a peak of 1,367 ± 33 nM, which subsequently declined over 10 min to a low sustained plateau of 227 ± 5 nM (means ± s.e.m., $n = 572$ cells) (Fig. 1a). The time course of NF-κB activation during this response was assayed by the phosphorylation and degradation of its cytoplasmic inhibitor IκBα, or by the accumulation of the NF-κB subunit, RelA, in the nucleus[7,16,17]. NF-κB activation was first detectable 4 min after stimulation with HEL and reached completion by 8 min (Fig. 1b). Like NF-κB activation, the phosphorylation of JNK1 and its nuclear substrate ATF-2 (refs 10, 18) was also first apparent within 4 min and reached a peak by 12 min (Fig. 1c). In contrast, activation of NFATc, as determined by its translocation to the nucleus, was much more rapid, being essentially complete within 1 min of stimulation with antigen (Fig. 1d, e). The activation of each of these pathways was inhibited by the immunosuppressant cyclosporin A (CsA)[19] as shown previously[8,9,20].

An important question is whether the spike and plateau phases of the Ca^{2+} response activate distinct transcriptional pathways. Stimulation of the antigen receptor activates Ca^{2+}-independent as well as Ca^{2+}-dependent signalling pathways[5,21]; we therefore applied the

Ca^{2+} ionophore ionomycin (in the presence of phorbol ester) to identify the specific impact of each phase of the Ca^{2+} response. The Ca^{2+} spike was generated in isolation by exposing the cells to ionomycin shortly before chelating extracellular Ca^{2+} with EGTA (Fig. 2a, left). Single-cell Ca^{2+} imaging confirmed that the ionomycin-induced transient had about the same magnitude as the HEL-stimulated spike (1,301 ± 46 nM versus 1,367 ± 33 nM, respectively; mean ± s.e.m.) and returned to baseline within 3 min. Furthermore, we verified that the Ca^{2+} spikes produced by HEL or ionomycin are attributable to Ca^{2+} released from internal stores (~25%) and to Ca^{2+} influx (~75%) (data not shown), indicating that ionomycin and HEL mobilize the same sources of Ca^{2+} to generate the spike. As a positive control, ionomycin was applied without EGTA to create a sustained $[Ca^{2+}]_i$ increase that fully activated all three pathways (Fig. 2a, right). Stimulation with phorbol ester alone did not raise $[Ca^{2+}]_i$ (data not shown), nor did it activate NFATc, NF-κB, or JNK1 (Fig. 1b–d, lanes marked P), confirming that all three pathways require elevated $[Ca^{2+}]_i$ for activation. In the absence of phorbol ester, Ca^{2+} ionophore alone did not activate NF-κB or JNK (ref. 19, and data not shown); ionomycin did cause nuclear translocation of NFATc but previous studies have shown that NFAT-dependent transcription requires a second signal that can be provided by protein kinase C[4,14].

The high-Ca^{2+} spike evoked prolonged activation of NF-κB and JNK1/ATF-2. IκBα became phosphorylated and was degraded within 4–8 min, and RelA accumulated in the nucleus with a parallel time course (Fig. 2b, e). The NF-κB response was comparable when $[Ca^{2+}]_i$ was raised continuously (Fig. 2b, e). Likewise, JNK1 and ATF-2 phosphorylation reached a stable maximum 8 min after the initial increase in $[Ca^{2+}]_i$, regardless of whether the rise was transient or sustained (Fig. 2c, e). Activation of both NF-κB and

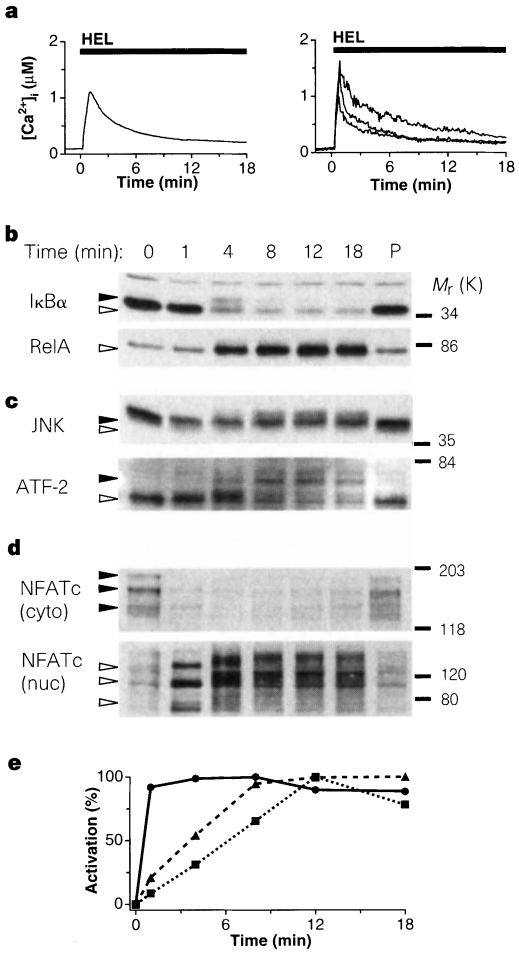

Figure 1 Antigen evokes a biphasic $[Ca^{2+}]_i$ rise that activates the NF-κB, JNK1 and NFAT pathways. **a**, Purified splenic B lymphocytes expressing a hen egg lysozyme(HEL)-specific immunoglobulin transgene were analysed by digital video microscopy. Fura-2-loaded cells were stimulated with 500 ng ml^{-1} HEL and 5 ng ml^{-1} phorbol 12,13-dibutyrate (PDBU) (bar). Mean responses of 285 cells (left) and of representative single cells (right) are shown. After stimulation, nuclear and cytoplasmic fractions were analysed by western blotting. **b**, NF-κB activation is demonstrated by the phosphorylation and degradation of cytoplasmic IκBα and the accumulation of RelA in nuclear lysates. Phosphorylated IκBα, first detectable at 4 min, has a slightly lower mobility than the dephosphorylated form. **c**, Cytoplasmic JNK1 and nuclear ATF-2 are phosphorylated following stimulation. Phosphorylation of JNK1 and ATF-2 causes a reduction in electrophoretic mobility[18] that is evident at 4–18 min. **d**, NFATc translocates rapidly from the cytoplasm (cyto) to the nucleus (nuc). NFATc in its phosphorylated state is present as several bands migrating with an apparent M_r of 160K–190K (filled arrows). Nuclear NFATc is dephosphorylated and migrates more rapidly (apparent M_r 80K–150K; open arrows). In **b**–**d**, lane P shows lysates from cells stimulated with 5 ng ml^{-1} PDBU alone for 12 min as a control. Time in min is indicated above each lane and the M_r values (in K) are shown on the right. Filled and open arrows indicate the positions of phosphorylated and unphosphorylated species, respectively. **e**, Time course of IκBα degradation (▲), JNK1 phosphorylation (■) and NFATc translocation (●) as determined by densitometry of the immunoblots in **b**–**d**.

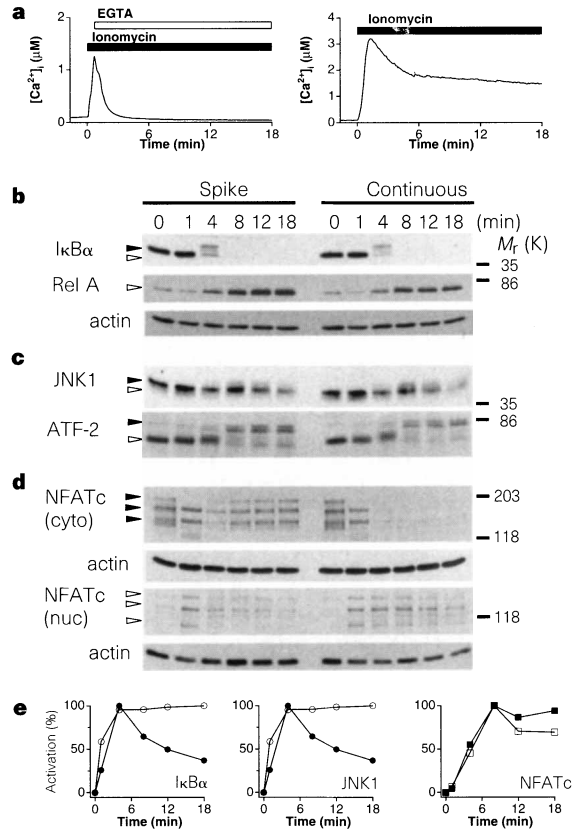

Figure 2 A brief Ca^{2+} spike induces persistent activation of NF-κB, JNK1 and ATF-2, but transient translocation of NFATc. **a**, Average Ca^{2+} response of >250 cells treated with 950 nM ionomycin and 5 ng ml^{-1} PDBU (black bar). Left, 3 mM EGTA was added 40 s later (white bar) to terminate the spike. **b**, The Ca^{2+} spike (left lanes) and the continuous $[Ca^{2+}]_i$ rise (right lanes) activate NF-κB similarly, as shown by IκBα phosphorylation and degradation and RelA translocation. **c**, JNK1 and ATF-2 phosphorylation are also sustained following an isolated Ca^{2+} spike or a prolonged $[Ca^{2+}]_i$ increase. **d**, Cytoplasmic NFATc (cyto) is dephosphorylated and enters the nucleus (nuc) but returns to the cytoplasm after $[Ca^{2+}]_i$ declines to baseline (left lanes). Continuously elevated $[Ca^{2+}]_i$ maintains NFATc in the nucleus (right lanes). **e**, Time course of IκBα degradation, JNK1 phosphorylation and NFATc translocation following the $[Ca^{2+}]_i$ spike (filled symbols) or the sustained $[Ca^{2+}]_i$ rise (open symbols). Data were from the experiment shown in **a**–**d**.

JNK1 was sustained for at least 16 min after termination of the $[Ca^{2+}]_i$ spike, indicating that both pathways retain a memory of transient $[Ca^{2+}]_i$ rises that outlasts the Ca^{2+} signal itself. By contrast, the Ca^{2+} spike evoked only a transient nuclear translocation of NFATc, with one half of the nuclear NFATc returning to the cytoplasm in its phosphorylated form 8 min after $[Ca^{2+}]_i$ returned to baseline (Fig. 2d, e). The reversal of nuclear translocation was caused by termination of the Ca^{2+} spike, because nuclear NFATc persisted in cells with constant elevated $[Ca^{2+}]_i$ (Fig. 2a, d). These results confirm and extend findings showing that NFAT requires a continuous $[Ca^{2+}]_i$ rise to remain localized in the nucleus[12,13]. They also demonstrate that differences in deactivation kinetics contribute to the differential activation of multiple transcriptional pathways by Ca^{2+}. Similar results were obtained when HEL followed by EGTA was used to generate an isolated Ca^{2+} spike (data not shown).

We next investigated whether the low-Ca^{2+} plateau triggered by antigen (Fig. 1) can evoke selective activation of transcriptional pathways. Small amounts of ionomycin were added stepwise in order to mimic the antigen-induced plateau without creating an initial spike (Fig. 3a). Low concentrations of ionomycin elicit Ca^{2+} influx in lymphocytes predominantly by activating store-operated Ca^{2+} channels that underlie the antigen-evoked $[Ca^{2+}]_i$ plateau[6]; thus ionomycin seems to mimic the Ca^{2+}-mobilizing action of antigen during the plateau as well as the spike. Stimulation of NF-κB or JNK1 was not detectable in response to the low-Ca^{2+} plateau (Fig. 3b), whereas NFATc was activated by 70% within 12 min, suggesting that the former are less Ca^{2+} responsive than NFATc. To examine the Ca^{2+} sensitivity of each pathway in more detail, we measured the activation of NF-κB, JNK1, NFATc and NFATp[14] following a 10-min stimulation with increasing concentrations of ionomycin. Consistent with the results shown in Fig. 3, nuclear translocation of NFATc/p was induced by lower concentrations of ionomycin (79 nM; Fig. 4a) than are required to activate IκBα degradation or JNK1/ATF-2 phosphorylation (400–600 nM; Fig. 4a). Figure 4c shows the translocation of NFATc/p, degradation of IκBα, and phosphorylation of JNK1 and ATF-2 as a function of the peak $[Ca^{2+}]_i$ evoked by different doses of ionomycin (Fig. 4b). The results identify a range of $[Ca^{2+}]_i$ levels (200–400 nM) that promote NFATc/p translocation without activating NF-κB or JNK1. In three experiments, the $[Ca^{2+}]_i$ needed to half-maximally translocate NFATc/p (413 ± 114 nM) was substantially lower than the level needed to attain half-maximal degradation of IκBα (612 ± 121 nM) or phosphorylation of JNK1 and ATF-2

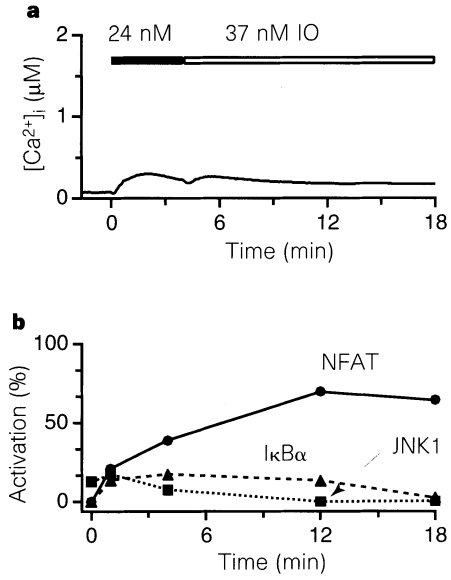

Figure 3 Selective activation of NFATc by a low $[Ca^{2+}]_i$ plateau. **a**, Cells were stimulated in the constant presence of 5 ng ml^{-1} PDBU with 24 nM ionomycin (IO) for 4 min, followed by addition of 37 nM ionomycin. The steady-state $[Ca^{2+}]_i$ plateau produced under these conditions simulates that induced by HEL stimulation (Fig. 1). **b**, Time course of NFATc translocation (●), IκBα degradation (▲), and JNK1 phosphorylation (■) for the experiment shown in **a**.

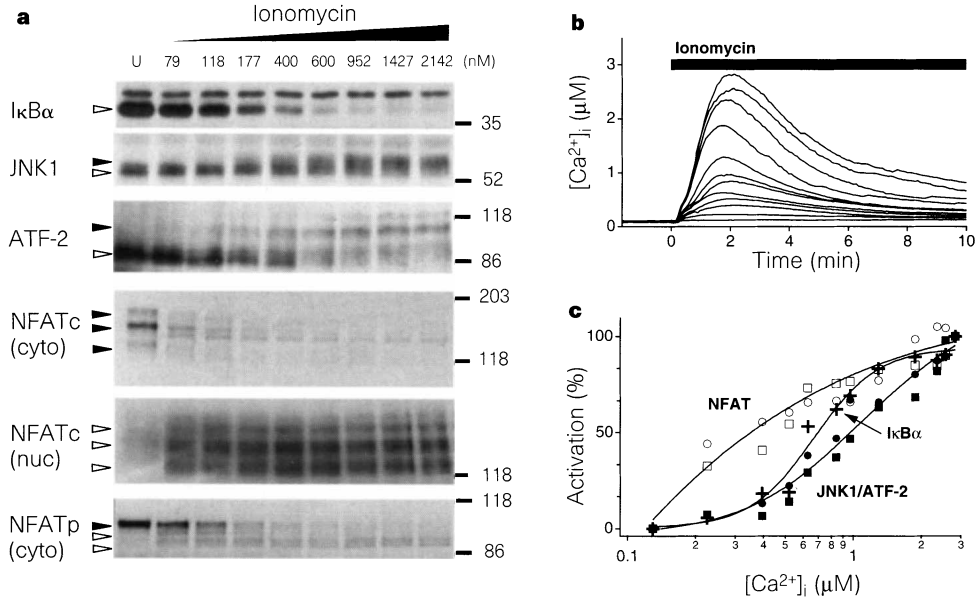

Figure 4 Differential Ca^{2+} sensitivity of NFATc/p, IκBα/RelA and JNK1/ATF-2. **a**, Cells were treated with increasing concentrations of ionomycin in the presence of 5 ng ml^{-1} PDBU and analysed by western blotting 10 min after stimulation. The concentration of ionomycin in nM is indicated above each lane (U, unstimulated). **b**, Average $[Ca^{2+}]_i$ responses of >250 cells stimulated with increasing doses of ionomycin (23, 35, 52 nM, in addition to the concentrations shown in **a**). The same batch of cells and incubation conditions were used as in **a**. **c**, Degradation of IκBα (+), phosphorylation of JNK1 (●) and ATF-2 (■), and translocation of NFATc (□) and NFATp (○) are shown as a function of peak $[Ca^{2+}]_i$ for each dose of ionomycin applied in **b**. Peak $[Ca^{2+}]_i$ is most relevant for NF-κB and JNK1 because they respond in a prolonged fashion to a transient $[Ca^{2+}]_i$ spike (Fig. 2). Because NFATc/p responds reversibly to increases in $[Ca^{2+}]_i$ (Fig. 2), this analysis may slightly underestimate the true Ca^{2+} sensitivity of NFATc/p. The graph identifies a range of $[Ca^{2+}]_i$ that selectively activates NFATc/p without appreciably stimulating NF-κB or JNK1/ATF-2.

(1,035 ± 263 nM; means ± s.e.m.). These measurements of the Ca^{2+} sensitivity of NFAT translocation agree with the reported sensitivity of an NFAT/AP1-dependent reporter gene[6,11]. The Ca^{2+} dependence of NF-κB and JNK was previously inferred only qualitatively from their stimulation by Ca^{2+} ionophore[9] or from inhibition by drugs like CsA that inhibit calcineurin[8]. Our results indicate that NFATc/p is significantly more Ca^{2+}-sensitive than NF-κB and JNK1/ATF-2, and that this enhanced Ca^{2+} sensitivity enables NFAT to be selectively activated by the low-Ca^{2+} plateau.

The ability of cells to react appropriately to a wide variety of environmental stimuli requires a high degree of specificity in signalling from the plasma membrane to the nucleus. It is remarkable that such specificity is achieved, given the relatively small number of second messenger pathways that exist. Many mechanisms have been proposed to explain transcriptional selectivity[22], but the contribution of different Ca^{2+} signals to specificity has not been previously recognized. Our results show that the amplitude and duration of dynamic Ca^{2+} signals contribute to transcriptional specificity, and that this is a direct consequence of the differing Ca^{2+} sensitivities and kinetic behaviour of NF-κB, JNK and NFAT. These differences may also predict frequency-specific effects of $[Ca^{2+}]_i$ oscillations on gene transcription, which have been implicated in neuronal differentiation[23].

Differential signalling by Ca^{2+} is likely be important in the regulation of immunity and inflammation. In self-tolerant B cells, basal $[Ca^{2+}]_i$ is moderately raised and NFAT is activated, but acute stimulation with antigen fails to generate a Ca^{2+} spike or activate the NF-κB or JNK1 pathways[19]. Similarly, elevation of basal $[Ca^{2+}]_i$ and the absence of an antigen-induced Ca^{2+} spike has been reported in T cells rendered anergic by an anti-CD3 monoclonal antibody[24] and in T cells that have differentiated to the anti-inflammatory T_H2 state[24,25]. Low-amplitude Ca^{2+} responses have also been implicated in the induction of T-cell anergy by altered peptide ligands[26]. Conversely, a high Ca^{2+} spike without a lower plateau is triggered during the inhibition of B-cell responses by the binding of immune complexes to the Fc receptor[27,28]. Our findings suggest that the functional consequences of these isolated Ca^{2+} spikes and plateaux, as well as of other Ca^{2+} signalling patterns such as oscillations and waves, may arise from the selective activation of transcriptional regulators. The importance of second messenger amplitude and duration in discriminating between different response pathways may prove to be a common theme in many cells. □

Methods

Calcium imaging. For single-cell calcium imaging, purified B cells[29] were incubated at 37° with 1 μM Fura-2/AM (Molecular Probes) for 15 min in phenol-red-deficient RPMI supplemented with 3% fetal bovine serum (FBS). After loading, cells were washed and maintained at room temperature in a 5% CO_2 atmosphere for up to 1 hour. Cells were plated on clean glass coverslips and imaged at 37 °C in phenol-red-deficient RPMI with 1% FBS. Ratiometric imaging was done on the heated stage of a Zeiss Axiovert 35 microscope using a 40 × oil-immersion objective (Zeiss Achrostigmat, NA 1.3), an intensified CCD camera (Hamamatsu) and a Videoprobe image processor (ETM Systems) essentially as described[30].

Quantitation of western blots. Cells were stimulated at a density of ~3 × 10^7 cells per ml in phenol-red-deficient RPMI with 1% FBS. Stimulations were stopped on ice, centrifuged and resuspended in hypotonic buffer (5 mM NaCl, 20 mM HEPES, pH 7.5) containing protease (2.5 mM PMSF, 40 μg ml^{-1} each of aprotinin and leupeptin, 2 mM EDTA) and phosphatase inhibitors (1 mM $NaVO_4$, 6 mM pNPP, 10 mM NaF) and 0.4% NP-40. Nuclei were separated by centrifugation at 600*g* at 3 °C and cytoplasmic extracts (supernatant) were added to boiling SDS–PAGE reducing sample buffer. Nuclei were rinsed in hypotonic buffer with inhibitors and lysed in boiling sample buffer. For Figs 1–3, chromatin was removed from nuclear extracts by centrifugation at 70,000*g* in a Beckman airfuge. For Fig. 4, chromatin was sheared by passing it repeatedly through a 26-gauge needle. Extracts were resolved by SDS–PAGE, transferred to nitrocellulose and analysed by immunoblot and ECL (Amersham). Anti-NFATc(7A6) and anti-NFATp(4G10G5) were obtained from L. Timmerman and G. Crabtree, anti-IκBα and anti-RelA were from Santa Cruz Biotechnology, anti-JNK1 was from Pharmingen and Santa Cruz Biotechnology, and anti-ATF was from J. Hoeffler and M. Green. Autoradiograms were analysed with a Molecular Dynamics computing densitometer using the volume-integrate mode. An exposed area of film outside each lane was used as background. Raw density values for NFATc, IκBα, and RelA were corrected for the loading of each lane; for JNK1 and ATF-2, the density of phosphorylated bands was calculated relative to the summed density of the phosphorylated and unphosphorylated bands. NFATc activation was calculated from the loss of cytoplasmic material (measurements based on accumulation of nuclear material gave similar results). Activation is expressed relative to the values observed in unstimulated (0%) and maximally stimulated (100%) cells. On an absolute scale, maximal NFATc/p translocation ranged from 75–90%, maximal IκBα degradation was 80–99%, nuclear RelA was induced maximally by fivefold, ATF-2 phosphorylation was 20–30%, and maximum JNK1 phosphorylation ranged from 50–60%.

Received 16 December 1996; accepted 6 March 1997.

1. Ghosh, A. & Greenberg, M. E. Calcium signaling in neurons: molecular mechanisms and cellular consequences. *Science* **268,** 239–247 (1995).
2. Berridge, M. J. Inositol trisphosphate and calcium signalling. *Nature* **361,** 315–325 (1993).
3. Clapham, D. E. Calcium signaling. *Cell* **80,** 259–268 (1995).
4. Crabtree, G. R. & Clipstone, N. A. Signal transmission between the plasma membrane and nucleus of T lymphocytes. *Annu. Rev. Biochem.* **63,** 1045–1083 (1994).
5. Gold, M. R. & DeFranco, A. L. Biochemistry of B lymphocyte activation. *Adv. Immunol.* **55,** 221–295 (1994).
6. Fanger, C. M., Hoth, M., Crabtree, G. R. & Lewis, R. S. Characterization of T cell mutants with defects in capacitative calcium entry: genetic evidence for the physiological roles of CRAC channels. *J. Cell Biol.* **131,** 655–667 (1995).
7. Bauerle, P. A. & Henkel, T. Function and activation of NF-κB in the immune system. *Annu. Rev. Immunol.* **12,** 141–179 (1994).
8. Frantz, B. *et al.* Calcineurin acts in synergy with PMA to inactivate I kappa B/MAD3, an inhibitor of NF-κB. *EMBO J.* **13,** 861–870 (1994).
9. Su, B. *et al.* JNK is involved in signal integration during costimulation of T lymphocytes. *Cell* **77,** 727–736 (1994).
10. Karin, M. & Hunter, T. Transcriptional control by protein phosphorylation: signal transmission from the cell surface to the nucleus. *Curr. .Biol.* **5,** 747–757 (1995).
11. Negulescu, P. A., Shastri, N. & Cahalan, M. D. Intracellular calcium dependence of gene expression in single T lymphocytes. *Proc. Natl Acad. Sci. USA* **91,** 2873–2877 (1994).
12. Timmerman, L. A., Clipstone, N. A., Ho, S. N., Northrop, J. P. & Crabtree, G. R. Rapid shuttling of NF-AT in discrimination of Ca^{2+} signals and immunosuppression. *Nature* **383,** 837–840 (1996).
13. Shibasaki, F., Price, E. R., Milan, D. & McKeon, F. Role of kinases and the phosphatase calcineurin in the nuclear shuttling of transcription factor NF-AT4. *Nature* **382,** 370–373 (1996).
14. Rao, A. NF-ATp: a transcription factor required for the coordinate induction of several cytokine genes. *Immunol. Today* **15,** 274–281 (1994).
15. Goodnow, C. C. *et al.* Altered immunoglobulin expression and functional silencing of self-reactive B lymphocytes in transgenic mice. *Nature* **334,** 676–682 (1988).
16. DiDonato, J. A., Mercurio, F. & Karin, M. Phosphorylation of I-κBα precedes but is not sufficient for its dissociation from NF-κB. *Mol. Cell. Biol.* **15,** 1302–1311 (1995).
17. Verma, I. M., Stevenson, J. K., Schwarz, E. M., Van Antwerp, D. & Miyamoto, S. Rel/NF-κB/IκB family: intimate tales of association and dissociation. *Genes Dev.* **9,** 2723–2735 (1995).
18. Gupta, S., Campbell, D., Dérijard, B. & Davis, R. J. Transcription factor ATF-2 regulation by the JNK signal transduction pathway. *Science* **267,** 389–393 (1995).
19. Healy, J. I. *et al.* Different nuclear signals are activated by the B cell receptor during positive versus negative signaling. *Immunity* (in the press).
20. Flanagan, W. M., Corthésy, B., Bram, R. J. & Crabtree, G. R. Nuclear association of a T-cell transcription factor blocked by FK506 and cyclosporin A. *Nature* **352,** 803–807 (1991).
21. Cambier, J. C., Pleiman, C. M. & Clark, M. R. Signal transduction by the B cell antigen receptor and its coreceptors. *Annu. Rev. Immunol.* **12,** 457–486 (1994).
22. Ernst, P. & Smale, S. T. Combinatorial regulation of transcription 1: general aspects of transcriptional control. *Immunity* **2,** 311–319 (1995).
23. Gu, X. & Spitzer, N. C. Distinct aspects of neuronal differentiation encoded by frequency of spontaneous Ca^{2+} transients. *Nature* **375,** 784–787 (1995).
24. Gajewski, T. F., Lancki, D. W., Stack, R. & Fitch, F. W. "Anergy" of TH0 helper T lymphocytes induces downregulation of TH1 characteristics and a transition to a TH2-like phenotype. *J. Exp. Med.* **179,** 481–491 (1994).
25. Gajewski, T. F., Schell, S. R. & Fitch, F. W. Evidence implicating utiilization of different T cell receptor-associated signaling pathways by TH1 and TH2 clones. *J. Immunol.* **144,** 4110–4120 (1990).
26. Sloan-Lancaster, J., Steinberg, T. H. & Allen, P. M. Selective activation of the calcium signaling pathway by altered peptide ligands. *J. Exp. Med.* **184,** 1525–1530 (1996).
27. Wilson, H. A. *et al.* The B lymphocyte calcium response to anti-Ig is diminished by membrane immunoglobulin cross-linkage to the Fc gamma receptor. *J. Immunol.* **138,** 1712–1718 (1987).
28. Choquet, D., Partiseti, M., Amigorena, S., Bonnerot, C. & Fridman, W. Cross-linking of IgG receptors inhibits membrane immunoglobulin-stimulated calcium influx in B lymphocytes. *J. Biol. Chem.* **121,** 355–363 (1993).
29. Cyster, J. *et al.* Regulation of B-lymphocyte negative and positive selection by tyrosine phosphatase CD45. *Nature* **381,** 325–328 (1996).
30. Dolmetsch, R. & Lewis, R. S. Signaling between intracellular Ca^{2+} stores and depletion-activated Ca^{2+} channels generates $[Ca^{2+}]_i$ oscillations in T lymphocytes. *J. Gen. Physiol.* **103,** 365–388 (1994).

Acknowledgements. We thank L. Timmerman, G. Crabtree, J. Hoeffler, and M. Green for the generous gifts of antibodies, and M. Hoth, A Zweifach, and R. Tsien for comments on an earlier version of the manuscript. R.E.D. is supported by an American Heart Association Fellowship, R.S.L. is supported by the NIH, C.C.G. is an investigator of the Howard Hughes Medical Institute, and J.I.H. is a Beckman Scholar supported by the NIGMS Medical Scientist Training Program.

Correspondence and requests for materials should be addressed to R.S.L. (e-mail: rslewis@leland.stanford.edu).